Open
ORIGINAL ARTICLE

Cell Research (2013) 23:1043-1054.

www.nature.com/cr

An ABA-mimicking ligand that reduces water loss and promotes drought resistance in plants

Minjie Cao[1, *], Xue Liu[1, 2, *], Yan Zhang[3], Xiaoqian Xue[3, 4], X Edward Zhou[5], Karsten Melcher[5], Pan Gao[1], Fuxing Wang[1], Liang Zeng[1], Yang Zhao[6], Yang Zhao[7], Pan Deng[8], Dafang Zhong[8], Jian-Kang Zhu[1, 6], H Eric Xu[2, 5], Yong Xu[3]

[1]Shanghai Center for Plant Stress Biology and Shanghai Institute of Plant Physiology and Ecology, Shanghai Institutes of Biological Sciences, Chinese Academy of Sciences, 300 Fenglin Road, Shanghai 200032, China; [2]VARI-SIMM Center, Center for Structure and Function of Drug Targets, Key Laboratory of Receptor Research, Shanghai Institute of Materia Medica, Chinese Academy of Sciences, Shanghai 201203, China; [3]Institute of Chemical Biology, Guangzhou Institutes of Biomedicine and Health, Chinese Academy of Sciences, No.190 Kaiyuan Avenue, Guangzhou Science Park, Guangzhou, Guangdong 510530, China; [4]Shenyang Pharmaceutical University, No.103 Wenhua Road, Shenhe District, Shenyang, Liaoning 110016, China; [5]Laboratory of Structural Sciences, Center for Structural Biology and Drug Discovery, Van Andel Research Institute, 333 Bostwick Ave., N.E., Grand Rapids, MI 49503, USA; [6]Department of Horticulture and Landscape Architecture, Purdue University, West Lafayette, IN 47906, USA; [7]Shanghai Institute of Plant Physiology and Ecology, Shanghai Institutes of Biological Sciences, Chinese Academy of Sciences, 300 Fenglin Road, Shanghai 200032, China; [8]Shanghai Institute of Materia Medica, Chinese Academy of Sciences, Shanghai 201203, China

Abscisic acid (ABA) is the most important hormone for plants to resist drought and other abiotic stresses. ABA binds directly to the PYR/PYL family of ABA receptors, resulting in inhibition of type 2C phosphatases (PP2C) and activation of downstream ABA signaling. It is envisioned that intervention of ABA signaling by small molecules could help plants to overcome abiotic stresses such as drought, cold and soil salinity. However, chemical instability and rapid catabolism by plant enzymes limit the practical application of ABA itself. Here we report the identification of a small molecule ABA mimic (AM1) that acts as a potent activator of multiple members of the family of ABA receptors. In *Arabidopsis*, AM1 activates a gene network that is highly similar to that induced by ABA. Treatments with AM1 inhibit seed germination, prevent leaf water loss, and promote drought resistance. We solved the crystal structure of AM1 in complex with the PYL2 ABA receptor and the HAB1 PP2C, which revealed that AM1 mediates a gate-latch-lock interacting network, a structural feature that is conserved in the ABA-bound receptor/PP2C complex. Together, these results demonstrate that a single small molecule ABA mimic can activate multiple ABA receptors and protect plants from water loss and drought stress. Moreover, the AM1 complex crystal structure provides a structural basis for designing the next generation of ABA-mimicking small molecules.

***Keywords*:** abscisic acid; plant hormone; drought resistance; crystal structure; ABA-mimicking ligand
Cell Research (2013) **23**:1043-1054. doi:10.1038/cr.2013.95; published online 9 July 2013

Introduction

The phytohormone ABA plays critical roles in regulating plant development, growth, and responses to abiotic stresses such as drought, salt, and cold [1]. The levels of ABA in plants are tightly controlled by the balance of biosynthesis and catabolism in response to environmental conditions [2]. Upon abiotic stresses, the levels of ABA can be elevated dramatically, leading to activation of ABA-responsive programs that allow plants to cope with stress conditions.

ABA signaling is initiated by the direct binding of ABA to a family of START domain proteins, designated as pyrabactin resistance 1 (PYR1) and 13 members of PYR1-like (PYL) proteins [3], also known as regulatory components of ABA receptors (RCARs) [4]. Upon ABA

*These two authors contributed equally to this work.
Correspondence: Jian-Kang Zhu[a], H Eric Xu[b], Yong Xu[c]
[a]E-mail: zhu132@purdue.edu
[b]E-mail: Eric.Xu@vai.org
[c]E-mail: xu_yong@gibh.ac.cn
Received 26 April 2013; revised 18 June 2013; accepted 3 July 2013; published online 9 July 2013

binding, these receptors increase their ability to bind and inhibit the clade A type 2C protein phosphatases (PP2Cs), including ABI1, ABI2 and HAB1. In the absence of ABA, these PP2Cs bind and inactivate subfamily 2 members of SNF1-related kinases (SnRK2 kinases) through dephosphorylation and physical block of the SnRK2 kinases [5, 6]. PP2C inhibition by ABA-bound receptors leads to activation of SnRK2s, which in turn phosphorylate and activate downstream effectors to switch on stress-response programs.

Structural studies have highlighted a conserved gate-latch-lock mechanism underlying ABA perception and signal transduction [7-11]. The apo ABA receptor contains an open ligand-binding pocket that is flanked by two highly conserved loops that serve as a gate and latch. ABA binding induces the closure of the ligand entry gate onto the latch, allowing the receptor to dock onto PP2Cs. A conserved tryptophan from the PP2C active site in turn inserts between the gate and latch and further locks the receptor-PP2C complex [7]. This tryptophan also functions as an ABA sensor through a water-mediated contact with the ketone group of ABA in the receptor pocket. Thus, the tryptophan lock of PP2Cs serves as an ABA sensor as well as a structural element that locks the ABA receptor/PP2C signaling complex [7, 12]. The residues that comprise the gate-latch-lock components are highly conserved across species, suggesting that this ABA signaling mechanism is conserved in economically important plants, including rice and maize [13].

Because of the central role of ABA in the adaptation of plants to abiotic stresses, it is envisioned that intervention of ABA signaling by small molecules could help plants to overcome abiotic stresses such as drought [14]. This is particularly important in the case for controlling water loss in economically important crops. Currently more than 70% of fresh water is used by agriculture, and in many arid areas fresh water has become the limiting factor for food production [15]. Because of its chemical instability, cost of production, and rapid catabolism by plant enzymes, ABA itself has few applications in

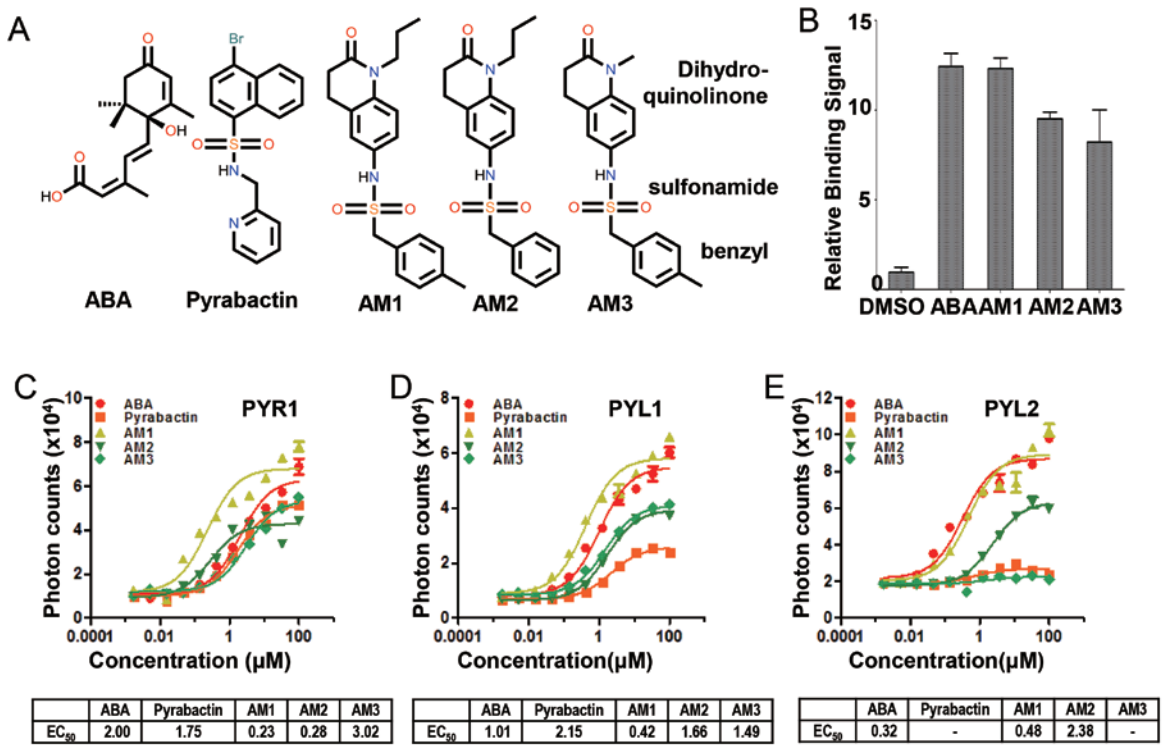

	ABA	Pyrabactin	AM1	AM2	AM3
EC_{50}	2.00	1.75	0.23	0.28	3.02

	ABA	Pyrabactin	AM1	AM2	AM3
EC_{50}	1.01	2.15	0.42	1.66	1.49

	ABA	Pyrabactin	AM1	AM2	AM3
EC_{50}	0.32	-	0.48	2.38	-

Figure 1 Chemical screening of ABA receptor agonist from small molecule library. **(A)** Two-dimensional chemical structures of AM1 (ABA mimics 1) and its analogs AM2, AM3. These compounds could be divided into three parts: dihydro-quinolinone hetero-ring head, sulfonamide linker and benzyl tail. **(B)** AlphaScreen interaction in the presence of 100 μM compound (*n* = 3, error bars = SD). 0.1% DMSO and 10 μM (+)-ABA are used as negative and positive controls, respectively. **(C-E)** Agonist dose response curves. Dose-dependent stimulation of the interaction between HAB1 and PYR1 **(C)**, PYL1 **(D)** or PYL2 **(E)** by (+)-ABA, Pyrabactin, and compounds AM1, AM2 and AM3 as determined by AlphaScreen assays. EC_{50} values for the interaction are listed below the curves (*n* = 3, error bars = SD).

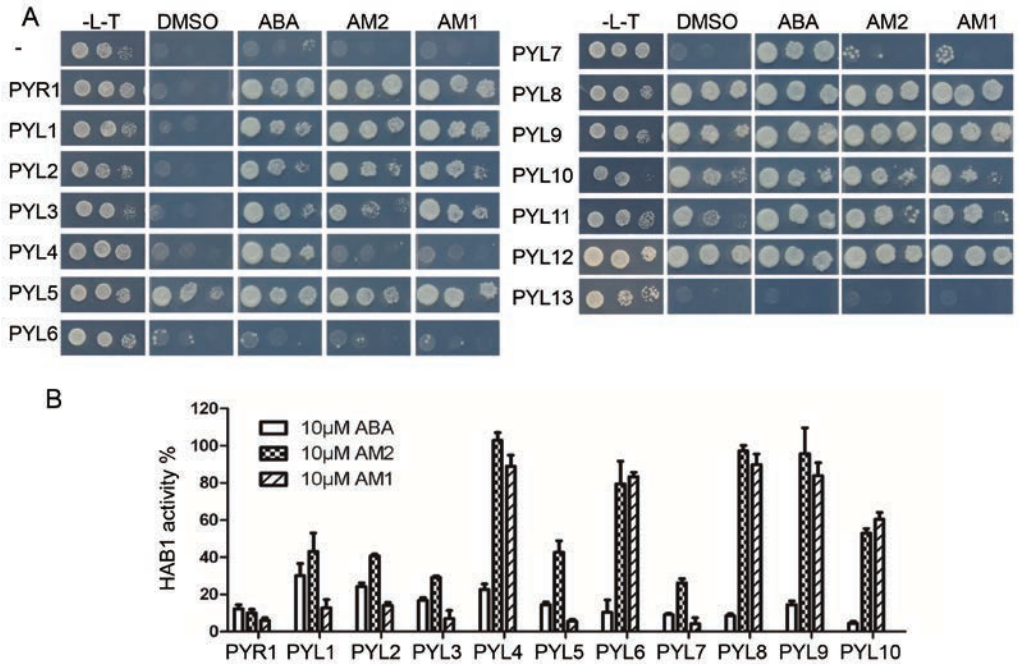

Figure 2 AM1 is a potent agonist of multiple ABA receptors. **(A)** Yeast-two-hybrid assay indicates that AM1 interacts with almost all ABA receptors. Interactions of 14 PYR/PYLs fused with binding domain (BD) with activation domain (AD)-fused HAB1 on -Leu/-Trp/-His SD media containing (+)-ABA and corresponding compounds were determined by yeast-two-hybrid assay. Working concentration is 10 μM for AM1, AM2 and (+)-ABA. -Leu/-Trp (-L/-T) and -Leu/-Trp/-His SD media containing 0.1% DMSO (DMSO) are used as positive and negative controls, respectively. **(B)** Agonist AM1 and AM2 induce HAB1 activity inhibition mediated by 11 PYLs, including PYR1 and PYL1-10, in phosphatase activity assay. Working concentration is 10 μM for AM1, AM2 and (+)-ABA. Values are means ± SD (*n* = 3).

actual agriculture practice. Thus, discovery of new ABA analogs that mimic ABA actions could lead to important agricultural applications and is a focus of the ABA research field. In this study, we identified and characterized a small molecule ABA mimic (AM1) that activates multiple ABA receptors and promotes drought resistance in *Arabidopsis*.

Result

Identification of ABA mimics

One hallmark of ABA signaling is ligand-mediated interaction between ABA receptors and PP2C phosphatases, which can be monitored by an AlphaScreen assay [3, 7]. In this assay, His-tagged PYR1 and biotin-tagged HAB1 were used to screen a small chemical library (~12 000 compounds, Life Chemical Inc.) for their ability to promote PYR1-HAB1 interactions (Supplementary information, Figure S1). From this screen, we identified three related sulfonamide compounds (Figure 1A), designated as ABA mimics 1-3 (AM1, 2, and 3), which have nearly the same ability as ABA to enhance PYR1-HAB1 interaction at 100 μM concentration (Figure 1B).

Pyrabactin is also a sulfonamide-based ABA analog, which was originally identified as a PYR1-specific activator [3], and was later characterized as an agonist of PYR1 and PYL1 but an antagonist of PYL2 [16]. Full dose response curves reveal that AM1 is more potent than ABA (8.7-fold) and Pyrabactin (7.6-fold), respectively, in promoting PYR1-HAB1 interaction, while AM2 and AM3 have relatively weaker potencies than AM1 (Figure 1C). Importantly, different from Pyrabactin, which is an antagonist of PYL2 [16], AM1-2 are full agonists of PYL1 and PYL2 (Figure 1D and 1E). The potency of AM1 to PYL2 is comparable to that of ABA, but to PYL1, AM1 is 2.4-fold more potent than ABA (Figure 1D and 1E). Among the three AM compounds, AM1 has the lowest EC50 and is 2.4- to 8.7-fold more potent than ABA in respect to their ability to induce HAB-binding of PYR1 (8.7-fold) and PYL1 (2.4-fold). Thus, we focused on AM1 in our studies below.

AM1 is a potent agonist of multiple ABA receptors

The ABA receptor family consists of 14 START domain proteins. To investigate the activity of AM1 to the

ABA receptor family, we performed yeast-two-hybrid assay using 14 PYR/PYL receptors and 4 clade A PP2C proteins (Figure 2A and Supplementary information, Figure S2). At 10 μM concentration, AM1 and AM2, similar to ABA, were able to promote the interaction of PYR1 and PYL1-3 (and to a lesser extent, PYL5 and PYL7) with HAB1 (Figure 2A). In contrast, at 2 μM concentration, AM2 failed to promote the interaction of ABA receptors with PP2Cs (Supplementary information, Figure S2). The results of PP2C inhibition experiments were consistent with the yeast-two-hybrid assays (Figure 2B). At 10 μM concentration, the HAB1 PP2C activity was inhibited by all receptor subtypes tested with ABA, consistent with ABA as a pan agonist of PYR/PYL receptors. Importantly, AM1 mediated potent inhibition of HAB1 when bound to six subtypes of ABA receptors (PYR1, PYL1, 2, 3, 5 and 7, Figure 2B). The degree of inhibition by AM1 was even more pronounced than that by ABA through these receptor subtypes, indicating that AM1 is a potent agonist of these six ABA receptor subtypes.

AM1 potently activates the ABA-induced stress-response programs

To assess the biological activity of AM1 in whole plants, we treated 10-day-old wild-type and *pyr1/pyl1/pyl4* triple mutant plants with AM compounds and ABA at 50 μM for 6 h. The transcriptional levels of six ABA-induced genes, whose functions range from abiotic stress response to ABA biosynthesis, were quantitated by real-time PCR (Figure 3A). All six ABA-inducible genes were dramatically activated by the ABA treatment in wild-type plants. AM1 activated a similar transcriptional profile to ABA in wild-type plants, whereas AM2 was a much weaker activator, consistent with its weak potency.

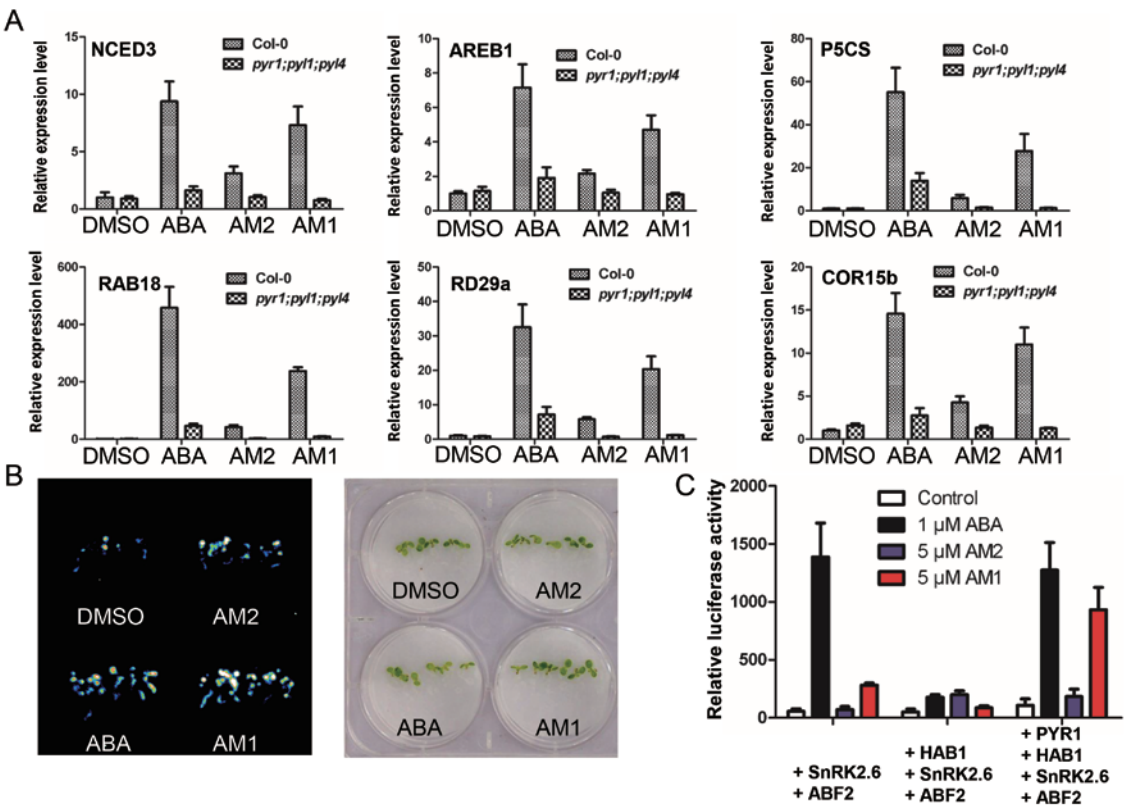

Figure 3 AM1 potently activates the ABA-induced stress-response programs. **(A)** Induction of abiotic stress-related gene expression of wild-type (Col-0) and *PYR*/*PYL* triple mutant (*pyr1;pyl1;pyl4*) after (+)-ABA, AM1 or AM2 treatment as determined by quantitative RT-PCR. Ten-day-old seedlings are treated with 50 μM compounds or (+)-ABA for another 6 h before RNA extraction, with 0.05% DMSO used as control. Values are means ± SD (*n* = 3). **(B)** Induction of luciferase expression in *pRD29a-LUC* reporter system. One-week-old seedlings grown on half-strength MS plates are transferred to filter paper soaked with 50 μM compounds or (+)-ABA for another 1.5 h before imaged for luminescence. 0.05% DMSO is used as control. **(C)** Activation of ABA signal transduction pathway by AM1 treatment. 5 μM AM1 dramatically activates reconstructed ABA signaling pathway (PYR1+HAB1+SnRK2.6+ABF2) in *pRD29b-LUC Arabidopsis* protoplasts when compared with AM2, and DMSO is used as control.

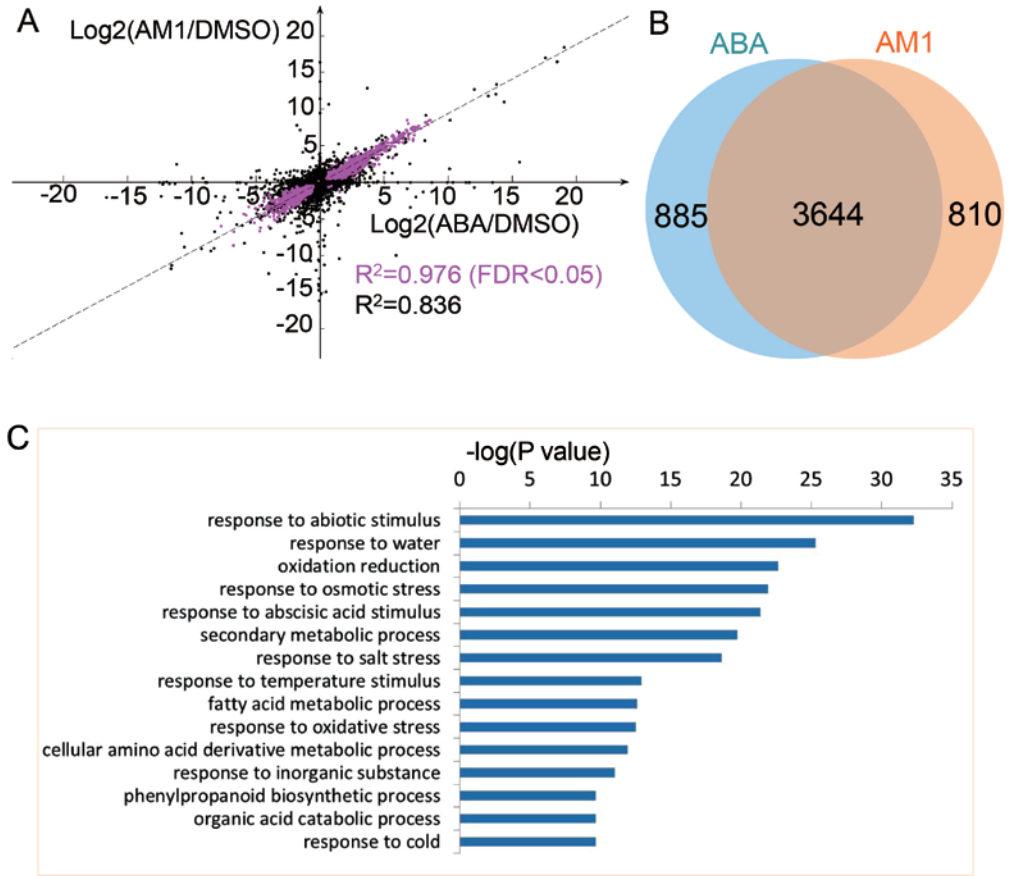

Figure 4 AM1 shows almost identical gene differential expression pattern to ABA. **(A)** AM1 and ABA induce highly correlated response at the transcriptional level. Scatters plot log_2-transformed values of differential expression genes (DEGs) responsive to AM1 (y axis) and ABA (x axis) treatment relative to DMSO control. Dots in black represent all the DEGs responsive to AM1 or ABA, while dots in purple represent the DEGs with a cut-off FDR < 0.05. The Spearman correlation coefficient (r) is shown in figure in corresponding colors. The *P*-value is less than 2×10^{-16} for AM1. **(B)** More than 80% DEGs overlap between AM1 and ABA treated samples. There are 4 529 genes up- or down-regulated after ABA treatment and 4 454 genes after AM1 treatment (FDR < 0.05). Among them, 3 644 genes are common in both treatments. **(C)** Ontology analysis of 3 644 DEGs responsive to both AM1 and ABA treatments. The most enriched biological processes based on their *P* values belong to abiotic stress response, as shown in Figure.

In *pyr1/pyl1/pyl4* triple mutant plants, the activation of the six genes by ABA was much reduced, but remained inducible by ABA, indicating that simultaneous disruption of PYR1, PYL1 and PYL4 remarkably attenuated ABA signal transduction in *Arabidopsis* seedlings and suggesting a critical role of these three PYR/PYL proteins in early stage of life cycle. The inductions of the ABA-inducible genes by AM1 and AM2 were nearly completely abolished in *pyr1/pyl1/pyl4* triple mutant plants, suggesting the crucial role of these three receptor subtypes in mediating AM1 and AM2 activity.

ABA-induced stress-response program can also be monitored in transgenic plants containing a firefly luciferase reporter driven by the *RD29a* promoter [17, 18]. As shown in Figure 3B, AM1 activated the *RD29a*-luciferase reporter as potently as ABA while AM2 activated the reporter to a lesser extent. This observation can be replicated in *snrk2.2/2.3/2.6* triple mutant protoplast cells transfected with expression plasmids for the PYR1 receptor, the HAB1 PP2C, the SnRK2.6 kinase, the ABF2 transcription factor, and the *RD29b*-luciferase reporter [19] (Figure 3C). Both AM1 and ABA efficiently activate the *RD29b*-luciferase reporter in this reconstituted system. In the absence of PYR1 transfection, AM1 can only activate a much lower level of *RD29b*-luciferase than ABA, which might be due to the fact that ABA is a pan agonist, thus is able to activate more subtypes of ABA receptors than AM1 in the protoplast assays.

To further correlate the biological activity of AM1 with ABA, we used RNA-seq to profile the transcriptome

of 10-day-old *Arabidopsis* seedlings treated with 50 μM of AM compounds and ABA. Both AM1 and ABA induced a highly correlated response in transcript levels [3] (R^2 = 0.976 with a cut-off FDR < 0.05) (Figure 4A), and this is in contrast to the low correlation between genes induced by Pyrabactin and ABA [3]. Compared with the DMSO control sample, 4 529 and 4 454 genes were identified to be induced by ABA and AM1, respectively, and among those, 3 644 genes (more than 80%) were common in samples treated with AM1 and ABA (Figure 4B). Gene ontology analysis of these genes reveals that abiotic stress-related biological processes were highly enriched by AM1 treatment, which strongly indicated a similar biological function of AM1 and ABA (Figure 4C).

AM1 treatments inhibit seed germination, reduce water loss and enhance drought resistance in Arabidopsis

One of the biological activities of ABA is to inhibit seed germination. As shown in Figure 5A, ABA treatments inhibit germination of wild-type Col-0 seeds and this inhibition can be completely abolished by simultaneous disruption of PYR1, PYL1, and PYL4 as reported previously, indicating that PYR1, PYL1, and PYL4 are the main contributor to ABA-induced inhibition of seed germination. Similarly, AM1 induces inhibition of seed germination at a level comparable to that of ABA in wild-type plants, whereas AM2 at the same concentration (1 μM) was inactive in this assay (Figure 5B). The *pyr1/pyl1/pyl4* triple mutations release AM1 inhibition of seed germination, suggesting that these three receptor subtypes play a large role in AM1-mediated inhibition of seed germination.

In addition to its effect on seed germination, AM1 treatments also induce responses of mature plants to abiotic stresses such as dehydration. Water loss of rosette leaves from one-month-old Col-0 plants was decreased after AM1 and ABA treatments when compared with DMSO treatments, while AM2 treatments showed no effect (Figure 6A). Consistent with the water loss result, AM1, instead of AM2, dramatically increased the drought resistance of plants. By maintaining more water, plants treated with AM1 successfully escaped from severe dehydration and rapidly recovered after re-watering (Figure 6B and 6C). These results clearly show that AM1 could function as an effective ABA analog during the vegetative growth stage.

Structural basis of AM1 recognition by ABA receptors

To understand the molecular basis of AM1 as an agonist of ABA receptors, we determined the crystal structure of AM1 bound to the PYL2-HAB1 complex at

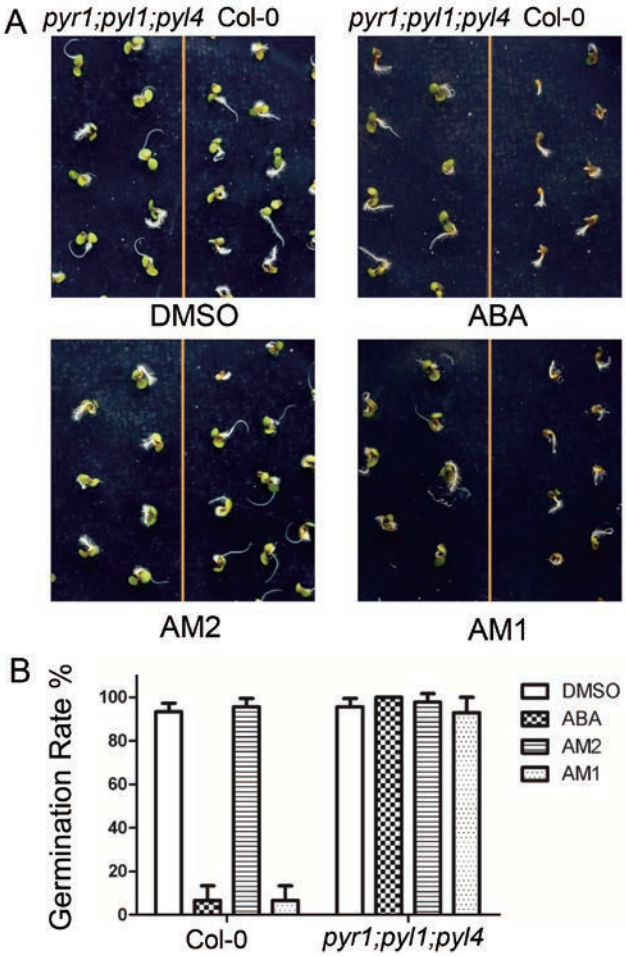

Figure 5 AM1 treatments inhibited seed germination. **(A-B)** Seeds of the wild type (Col-0) and *PYR*/*PYL* triple mutant (*pyr1;pyl1;pyl4*) are shown on half-strength MS (1% sucrose) plate containing corresponding compounds. Working concentration is 1 μM for both chemicals and (+)-ABA, and 0.1% DMSO is used as control. Seeds are considered germinated when green cotyledons expand. Photographs **A** are imaged and germination frequencies **B** are counted 4 days post triple mutant seed germination. Values are the mean germination frequency from four separate plates (15 seeds per plate) for each line. Error bars indicate SD.

a resolution of 2.88 Å. For structural comparison, we also determined the crystal structures of AM2 and AM3 bound to the PYL2-HAB1 complex at resolutions of 2.70 Å and 3.15 Å, respectively. We solved these structures by molecular replacement using the PYL1-ABA-ABI1 structure (PDB:3KB3) [7] as an initial model with the statistics of data and structures summarized in Supplementary information, Table S1. All three complexes share the same P212121 space group. Supplementary information, Figure S3 shows the overall arrangement

of the PYL2-AM1-HAB1 structure. The binding mode of AM1 is clearly defined by the electron density map in Figure 7A. AM1 is centered in the pocket with its dihydro-quinolinone ring, sulfonamide group and benzyl group fitting snugly into the hydrophobic pocket of PYL2. The intermolecular interactions between AM1 and PYL2 are diagramed in Figure 7B. The carbonyl oxygen on the dihydro-quinolinone ring forms a water-mediated hydrogen bond with residue Trp385 from HAB1. The N-substituted propyl group plugs into a narrow hydrophobic hole formed by residues Phe66, Leu91, Phe165, and Val169 along the wall and Val393 from HAB1 at the bottom. The sulfonamide group forms several hydrogen bonds with the side chains of the charged residues Lys64 and Glu98 (Figure 7B and 7C). The methyl benzyl group makes interactions with Tyr124, Val166, Val169 and Val170. AM2 and AM3 adopt a similar structure to that of AM1 (Supplementary information, Figure S4). However, compared to AM1, AM2 and AM3 lack the para-methyl group and the propyl group from the dihydro-quinolinone ring, both of which in the AM1 complex structure make snug interactions with the PYL2 receptor, thus providing a structural basis for the higher binding affinity of AM1 compared to those of AM2 and AM3.

Structural comparisons of the binding mode of AM1 with those of ABA and Pyrabactin revealed interesting similarities to ABA and differences to Pyrabactin (Figure 8). The overall arrangement of the PYL2-AM1-HAB1 complex resembles the agonist structure of the PYL2-ABA-HAB1 complex, with the gate and latch loops of PYL2 adopting the closed conformation that is further stabilized by the insertion of the locking residue, Trp385

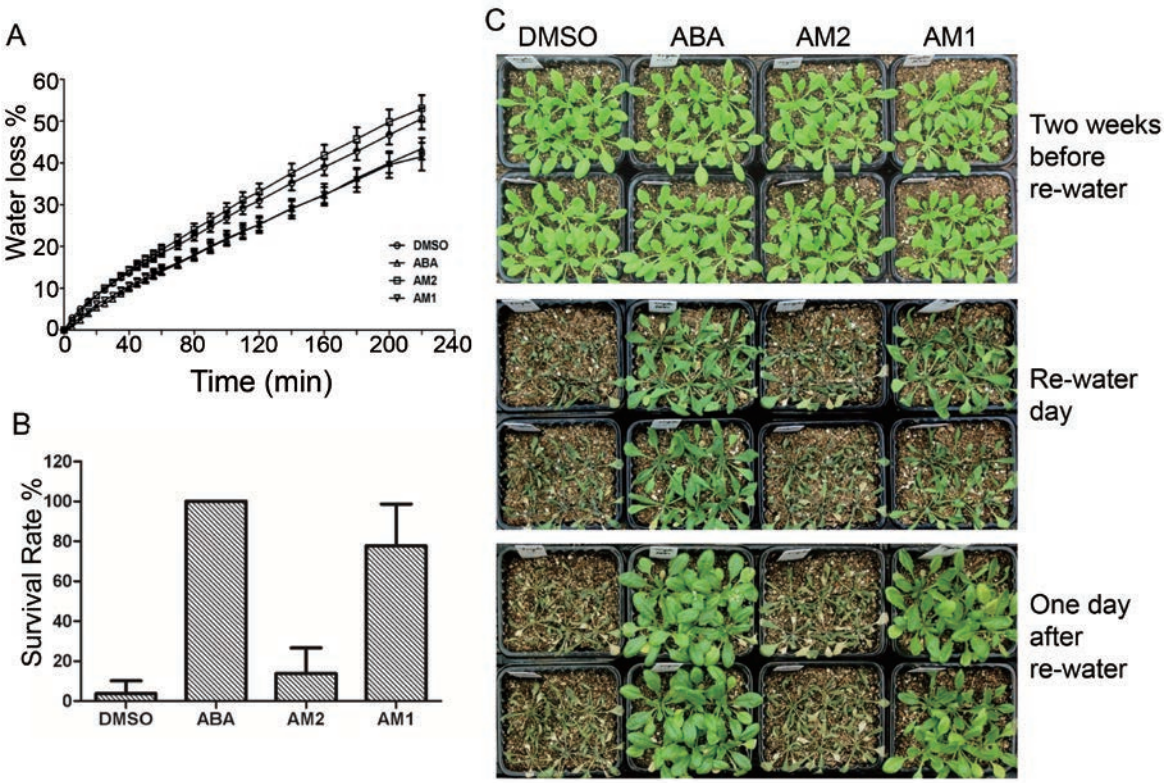

Figure 6 AM1 treatment reduced water loss and enhanced drought resistance. **(A)** Rapid dehydration of detached rosettes from 4-week-old plants. Well-irrigated plants are sprayed with AM1, AM2 or (+)-ABA solutions and rosette leaves of identical size are cut off 3 h after treatment. The working concentration was 50 μM for both compounds and (+)-ABA, and all sprays were added 0.02% Tween-20. 0.1% DMSO is used as control. Water loss rate is determined as % of initial fresh weight. Error bars represent standard error values (*n* = 4). **(B-C)** Drought stress assay. Wild-type (Col-0) plants are grown under short-day condition described in Materials and Methods for two weeks before water withdrawal. Then plants are sprayed with AM1, AM2 or (+)-ABA solutions used in rapid dehydration assay every other day for another two weeks before re-watering. 0.1% DMSO is used as control. Photographs in **C** were imaged before water withdrawal (top panel), before (middle panel) and one-day after re-watering (bottom panel). And survival rates in **B** were calculated one day after re-watering. Values are the mean survival rates from three independent assays (24 seedlings per assay). Error bars indicate SD.

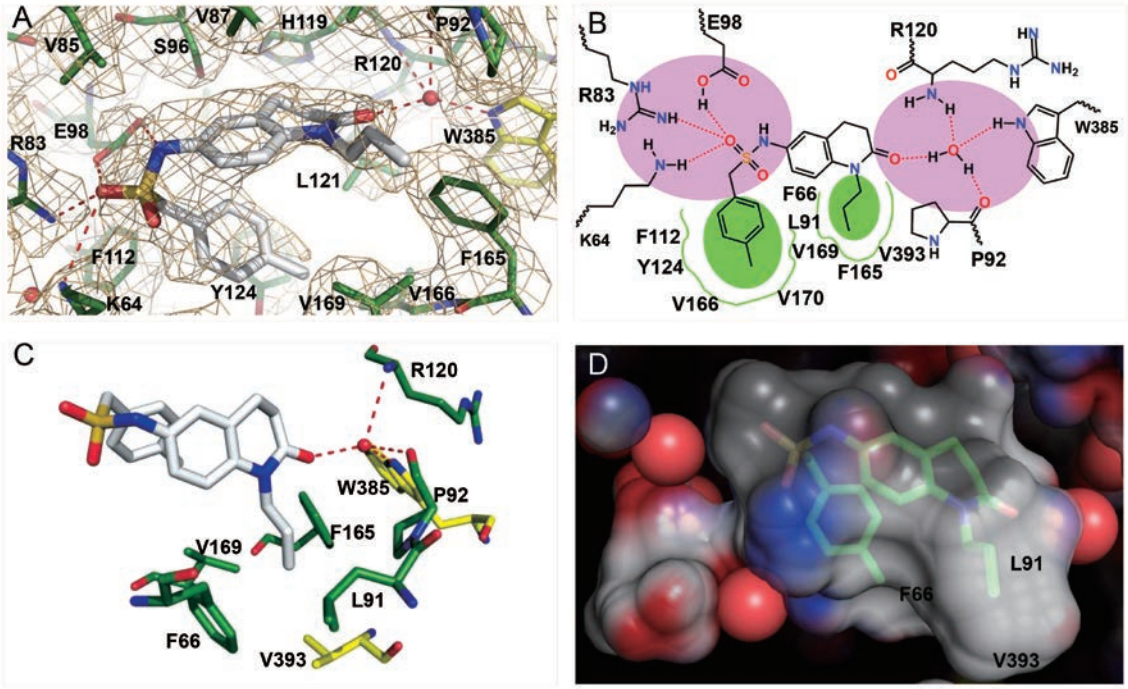

Figure 7 Structure determination of the PYL2-agonist-HAB1 complex. **(A)** $2F_o$-F_c composite omit electron density map of bound AM1 and its surrounding residues contoured at 1.0 σ. **(B)** Schematic presentation of the interactions between PYL2 binding pocket residues and the bound AM1. Charged interactions and hydrogen bonds are indicated by dash lines (red), hydrophobic interactions by solid lines (green). **(C)** N-substituted propyl is surrounded by hydrophobic residues Phe66, Leu91, Phe165, Val169 and Val393. **(D)** Active site inner surface is shown as electrostatic potential. Propyl group snugly plug into the hydrophobic sub-pocket.

from HAB1 (Figure 7). The binding mode of AM1 mimics that of ABA, with the carbonyl head group of AM1 overlapping extensively with the carbonyl head group of ABA, both of them forming a water-mediated hydrogen bond with Trp385. As mentioned in our previous study [7], this carbonyl head on the dihydro-quinolinone ring is critical to anchor the ligand in the active site, which is completely absent in the Pyrabactin structure. The sulfonamide group, which is reversed from the sulfonamide moiety of Pyrabactin, is located in the hydrophilic part of the pocket and makes direct hydrogen bond interactions with Glu98 and Lys64 (Figure 7). In the PYL2-HAB1-ABA structure, ABA forms two water-mediated hydrogen bonds with residue Glu98. The acid head group forms a charged interaction with the side chain of Lys64 (Figures 7 and 8). Several water-mediated hydrogen bonds in the ABA-bound complex are replaced by one of the oxygen atoms from the sulfonamide group in AM1. This can be explained by the favorable electrostatic and hydrogen-bond interactions made by the sulfonamide group. Interestingly, seven well-ordered water molecules present for ABA in the hydrophilic part of the pocket have been displaced in the complex with AM1 (Figures 7 and 8). The similar binding mode of AM1 to that of ABA thus provides a structural explanation for their shared biological activities in activating stress-response programs in plants.

Discussion

In this paper, we identified a small molecule ABA mimic, AM1, which acts as a potent agonist for multiple ABA receptors. Although both AM1 and Pyrabactin belong to the sulfonamide class of compounds (Figure 1A), the two compounds are quite different in their biological activities. Previous studies indicated that Pyrabactin is a selective agonist of PYR1 [3] and a weak agonist of PYL1, but it is an antagonist of PYL2 [16]. Thus, Pyrabactin is mainly active as an inhibitor of seed germination but it is inactive in the vegetative stage and fails to prevent water loss in plants [3]. In contrast, AM1 contains two important chemical moieties that make it distinct from Pyrabactin. The first moiety is the ketone oxygen, which mimics the cyclohexenone oxygen of

ABA. This is a critical chemical motif in ABA that forms a water-mediated hydrogen bond with the "tryptophan lock" of the PP2C, which is required for stabilizing the ligand-bound receptor/PP2C signaling complex [7]. The ketone oxygen moiety is absent in Pyrabactin. The second moiety is the sulfonamide group in AM1, which is in a reverse orientation relative to Pyrabactin (Figure 1A). The structure reveals that the AM1 sulfonamide group resembles the carboxylate group of ABA by making direct hydrogen bonds with Lys64 as well as residues Arg83 and Glu98 (Figure 7B). Thus, AM1 structurally and functionally mimics ABA, making AM1 capable of preventing plants from water loss and eliciting drought resistance.

There are a number of differences between AM1 and ABA. The first difference is that ABA is a pan agonist of the PYR/PYL family of receptors while AM1 is an agonist for a selective subset of ABA receptors (PYR1, PYL1, 2, 3, 5, and 7) (Figure 2B). In both germination assays and water loss experiments, AM1 and ABA show little difference, suggesting that the above subset of receptors may be the key players in controlling both seed germination and leaf transpiration in plants. However, there may be subtle functional differences between AM1 and ABA activities that were not detected in our current studies due to their different abilities to activate different receptors. The second difference is that AM1 and ABA have different potencies in activation of individual ABA receptors. In both AlphaScreen protein interaction and PP2C inhibition assays, AM1 is more potent than ABA for the above subset of ABA receptors (Figures 1C and 2B). However, the potency of AM1 in seed germination and water loss experiments is about the same, but not better than that of ABA. This discrepancy may result from different receptor activation profiles of AM1 and ABA. For example, PYL4 is activated by ABA but not AM1. As promoting drought resistance will be one of the major applications of ABA mimics, it will be particularly interesting to determine the expression profiles of ABA receptors in guard cells, and then design pan agonists against ABA receptors in guard cells.

We also speculate that there may be some difference in chemical stabilities between AM1 and ABA. ABA is well-known to be metabolically unstable due to glycosylation at its carboxylate group and hydroxylation at its cyclohexenone ring [20, 21]. ABA is also light sensitive due to the conjugated linker between its carboxylate and cyclohexenone ring (Figure 1A). The instability of ABA

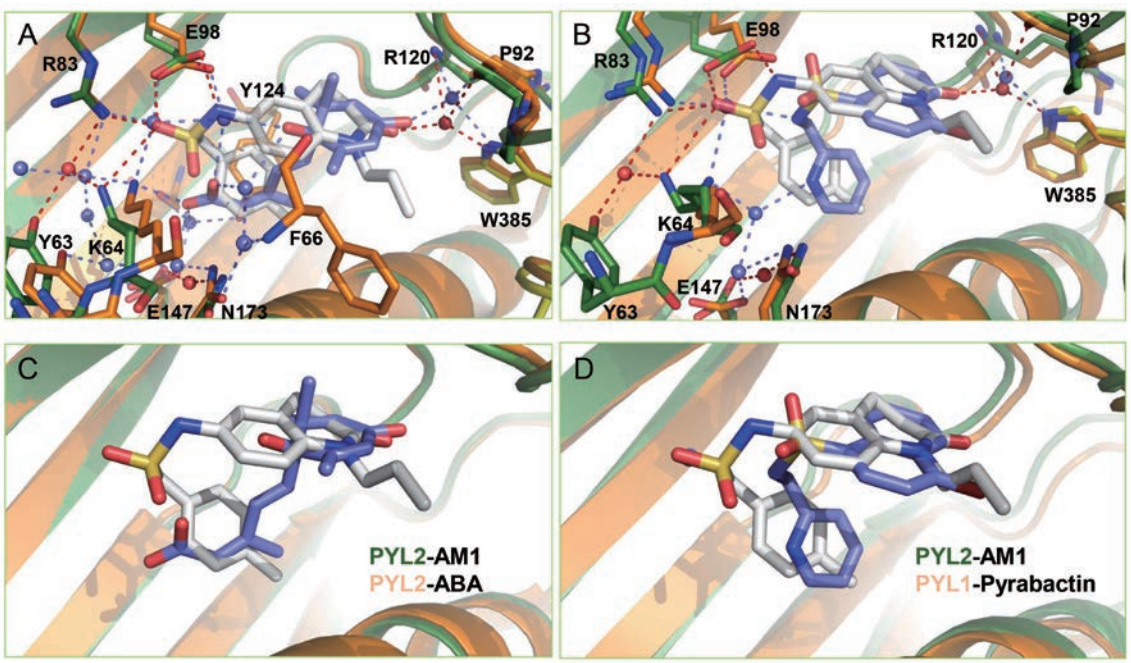

Figure 8 Structural comparison of diverse agonists with ABA receptor. **(A**, **C)** Overlay of AM1 (white) with ABA (slate blue) (PDB:3KB3) in the PYL2 binding pocket. Water molecules were shown in red in PYL2-AM1-HAB1 structure and in slate in PYL2-ABA-HAB1 structure. **(B**, **D)** Overlay of AM1 (white) in the PYL2 binding pocket with Pyrabactin (slate blue) (PDB: 3NMN) in the PYR1 binding pocket. Water molecules were shown in red in PYL2-AM1-HAB1 structure and in slate in PYL1-Pyrabactin-ABI1 structure.

is the main reason that limits ABA application. AM1 lacks the carboxylate group as well as the conjugated linker, we thus speculate that AM1 is chemically more stable. Indeed, when exposed to mild UV light, ABA has a half-life of only 24 min while the half-life of AM1 is 174 min, about 7-fold longer than ABA (Supplementary information, Figure S5), supporting that AM1 is chemically more stable than ABA. The detailed DMPK (drug metabolism and pharmacokinetics) profile of AM1 will require extensive future studies. Our results as reported here nevertheless provide a proof of concept that chemical ligands that activate multiple ABA receptors can be developed to protect plants from water loss and promote drought resistance. Given the highly conserved nature of ABA receptors and their signaling mechanisms in crop plants [13], we reason that such chemical ligands could have similar applications in economically important crops.

In addition to AM1, we also identified AM2 and AM3, two related sulfonamide compounds in our study. Compared to AM1, AM2 lacks the para-methyl group from the benzyl ring whereas AM3 lacks the propyl group from the dihydro-quinolinone ring. Such subtle structural differences have dramatic impacts on their biological activities. In most plant assays, AM1 mimics the functions of ABA. In contrast, AM2 is inactive in these assays (Figure 6). Structural comparisons of AM1, AM2 and AM3 reveal that both the para-methyl group and the propyl group of AM1 make close hydrophobic interactions with the PYL2 receptor. The availability of all three AM-bound structures thus provides a detailed structural basis to explain the delicate structure-activity relationship of these ABA mimics, and a rational framework for designing the next generation of ABA analogs for applications in drought stress management for agricultural crops.

Materials and Methods

Chemicals

Small molecule library with ~12 000 compounds were chosen based on chemical diversity and ordered from Life Chemical Inc. The Life Chemicals IDs for AM1 and its analogues AM2, AM3 are F2385-0086, F2385-0083 and F2278-0186, respectively. (+)-ABA and Pyrabactin were ordered from A. G. Scientific and Sigma, respectively. All compounds were diluted to 100 mM with DMSO for storage.

Protein preparation

PYR1 (residues 9-182), PYL1 (residues 36-211) and PYL2 (residues 14-188) and HAB1 (residues 172-511) were expressed in *E. Coli* BL21 (DE3) as H6-SUMO fusion proteins and purified following the same general methods as described [7]. Biotinylated PP2C protein HAB1 (residues 172-511) was prepared as recombinant fusion protein with Biotin-MBP tag for AlphaScreen assay and phosphatase activity assay.

AlphaScreen Assay

Interactions between PYR1/PYL1/PYL2 and HAB1 (PP2C) were assessed by luminescence-based AlphaScreen technology (Perkin Elmer) as previously described [6, 7, 16]. All reactions contained 100 nM recombinant H6-SUMO-PYR/PYL proteins bound to nickel-acceptor beads and 100 nM recombinant biotin-MBP-PP2C bound to streptavidin-acceptor beads in the presence and absence of the indicated amounts of (+)-ABA, Pyrabactin and compounds AM1, AM2, AM3. For dose-response assay, the concentration of (+)-ABA and compounds varied from 2 nM to 100 μM.

Crystallization, data collection and structure determination

To prepare the protein-ligand-PP2C ternary complex, we added ligand and purified PYL2 to purified HAB1 at a 5:1:1 molar ratio in the presence of 5 mM $MgCl_2$. PYL2-AM1-HAB1 complex crystals were grown at room temperature (20 ºC) in hanging drops containing 1.0 μl of the purified PYL2 protein and 1.0 μl of well solution containing 0.1 M Succinic acid and 15% PEG3350. For AM2 and AM3 complexes, the well solution containing 0.2 M ammonium sulphate, 0.1 M BIS-Tris pH 6.0, 25% PEG 3350. All crystals appeared within 1 day and grew to a dimension of 100-120 μm within 3-4 days. Crystals were flash frozen in liquid nitrogen. All diffraction data were collected at 100 K using an X-ray beam at BL17U beamline at Shanghai Synchrotron Radiation Facilities. The observed reflections were reduced, merged and scaled with DENZO and SCALEPACK in the HKL2000 package [22]. Molecular replacement was performed using the Collaborative Computational Project 4 program Phaser [23]. Programs O [24] and Coot [25] were used to manually fit the protein model. Model refinement was performed with CNS [26] and the CCP4 program Refmac5 [27].

Plants materials and growth conditions

Arabidopsis thaliana ecotype Columbia-0 (Col-0), PYR/PYL triple mutant (*pyr1;pyl1;pyl4*) and p*RD29a*-luciferase (C24 background) plant used in germination assay and gene expression analysis were grown on half-strength MS (Murashige and Skoog) solid media containing 1% sucrose in an environment-controlled chamber at 22 °C with a photosynthetically active radiation of 75 $\mu mol/m^2/s^1$ and a day/night cycle of 16-h light/8-h dark. And Col-0 used in desiccation and water loss assays and p*RD29b*-luciferase (*snrk2.2/2.3/2.6* background) plant used in protoplast transactivation assay were grown on soil with a day/night cycle of 8-h light/16-h dark.

HAB1 phosphatase activity assay

100 nM Biotin-MBP-HAB1 and 500 nM corresponding H6-SUMO tagged PYR/PYLs were pre-incubated in 50 mM imidazole, pH 7.2, 5 mM $MgCl_2$, 0.1% β-mercaptoethanol and 0.5 μg/ml BSA for 30 min at room temperature, as described before [7]. An 11-amino acid phosphopeptide (HSQPKpSTVGTP), belonging to amino acids 170-180 of SnRK2.6 with Ser175 phosphorylated, was used as substrate of HAB1 phosphatase. Reactions were started by addition of 100 μM phosphopeptide, and phosphate released from the phosphopeptide was determined by colorimetric assay (BioVision) 20 min later.

Yeast-two-hybrid assay

Yeast-two-hybrid assay was carried out as described before [4, 7]. Open reading frames of 14 PYR/PYLs and four PP2Cs were amplified from cDNA of Col-0 plants by PCR and cloned into pBD-GAL4 Cam vector (Stratagene) and pGADT7 vector (Clontech), respectively. The vectors were confirmed by sequencing and co-transformed into yeast strain AH109 (Clontech) with corresponding PYR/PYL and PP2C vector combinations. After two days incubation at 30 °C, well-grown clones were rescued and diluted to OD_{600} = 0.3, which was further diluted to 1:5 and 1:25 dilution gradients. 1 μl dilution was added in SD agar plates lacking Leu, Trp and His (-L/-T/-H), but containing 1 mM 3-AT and 2 μM ABA, AM1 or AM2 compound, with -L/-T/-H SD agar plates containing 1 mM 3-AT and 1:5 000 diluted DMSO and -L/-T SD agar plates used as negative and positive control, respectively. Three independent assays using different clones were carried out and plates were incubated at 30 °C for another two days before photograph.

Gene expression analysis

RNA extraction, quantitative real-time PCR (qRT-PCR), RNA sequencing (RNA-seq) and data analysis 10-day-old seedlings of Col-0 wild-type plants grown on half strength MS solid media were treated with 0.05% DMSO, 50 μM corresponding compound or (+)-ABA for another 6 h before RNA extraction. Total RNAs were extracted using TRIzol (Invitrogen) method and RNase-free DNase (Qiagen) was used to remove the contaminating DNA before qRT-PCR and RNA-seq. For quantitative RT-PCR, total RNAs were reverse-transcribed with the TransScript RT kit (Invitrogen) according to the manufacturer's protocol. All quantitative RT-PCR assays were performed following two-step protocol of SYBR Premix Ex Taq™ II kit (TaKaRa) in a CFX96 Realtime system (BIO-RAD) as described in the manufacturer's instruction. Each assay consisted of three biological replicas and was performed twice. *ACT7* was used as internal control in quantitative RT-PCR.

Duplicate biological replicate samples were used for DMSO, compounds and ABA treatment. Total RNA samples were sequenced by Majorbio technology Inc. using Illumina HiSeq2000, with 10 M reads per sample with average length > 49 bp. Significance analysis of RNA-seq data was used to identify those genes significantly up- or down-regulated by treatments using unlogged data, with a false discovery rate (FDR) less than 0.05. Fold-change was computed with average transcript levels compared to DMSO control values, which was in turn $\log_2$-transformed and computed for Spearman Correlation Coefficients between samples. Differential genes expression was calculated by SAM analysis.

p*RD29a*-luciferase expression system Luciferase expression system p*RD29a*-LUC (C24 ecotype) widely used in our lab [17, 18] was used to identify the ABA-responsive gene expression. One-week-old seedlings grown on half strength MS solid media were transferred to filter paper soaked with 0.05% DMSO, 50 μM corresponding compound or (+)-ABA for another 1.5 h and luciferase imaging was carried out as described before [17, 18].

Protoplast transactivation assay 4-week-old plants grown on Jiffy7 soil pellets (Jiffy Products) were used for protoplast isolation. Protoplast isolation and transfection were carried out as described before [7, 19]. The luciferase promoted by *RD29b* promoter was used as ABA-responsive reporter gene.

Germination, desiccation assays and water loss

Germination assay was carried out as follows. Seeds of Col-0 and PYR/PYL triple mutant (*pyr1;pyl1;pyl4*) were stratified for 4 days before sowed on half strength MS solid media containing 1% sucrose and 1 μM corresponding compound or (+)-ABA, with 15 seeds per line per 6 cm plate and 4 plates for each chemical. The plates were kept in growth chamber at 22 °C under long-day condition. Seeds were evaluated from day-to-day and considered germinated when the green cotyledons expand. 0.05% DMSO was used as control.

4-day-old Col-0 wild-type plants of identical size grown on half strength MS solid media were transferred to soil and grown under short day condition for another ten days. Plants were then withheld water and sprayed with chemical solutions, each containing 50 μM corresponding compound and 0.02% Tween-20, every other day. 0.05% DMSO was used as control. Each pod had equivalent soils and plants and the position of pods and plates were changed every other day to minimize experimental error. After 12-14 days desiccation, the plants were re-watered and the survival rates were counted.

Well-irritated 4-week-old plants grown in soil were sprayed with solutions used in the desiccation assay and sent back to grown chamber for another 3 h. Rossete leaves of identical size and stage were severed and fresh weight was weighed before and after exposed in air. The interval of each count was 5 min in the first hour and extended to 10 min in the second hour.

Stability measurement of ABA and AM1

ABA and AM1 were dissolved in pure water at 100 μM and aliquots of 200 μl of these compound solutions were exposed to a UV light (8 W) under biochemical safety hood. At the indicated time points, one aliquot was withdrawn and was subjected to LC-MS analysis. The amount of ABA and AM1 was quantitated by their corresponding peaks in the LC-MS profiles and the half-life of ABA and AM1 was calculated based on the disappearance of the corresponding peaks.

Data deposition

The structure factors and atomic coordinates discussed in this work have been deposited in the Protein Data Bank (www.pdb.org). The accession codes are: 4LG5 for PYL2-AM1-HAB1, 4LGA for PYL2-AM2-HAB1, 4LGB for PYL2-AM3-HAB1.

Acknowledgments

This work was supported by the Jay and Betty Van Andel Foundation, Amway (China) (to H E X), the National Natural Science Foundation of China (NSFC 91217311, to H E X), US National Institute of Health (R01GM102545, to K M), Funding for the Shanghai Center for Plant Stress Biology supported by Chinese Academy of Sciences (to J-K Z), and the 100-talent program of Chinese Academy of Sciences (to Y X).

References

1 Zhu JK. Salt and drought stress signal transduction in plants. *Annu Rev Plant Biol* 2002; **53**:247-273.

2 Xiong L, Zhu JK. Regulation of abscisic acid biosynthesis. *Plant Physiol* 2003; **133**:29-36.
3 Park SY, Fung P, Nishimura N, *et al.* Abscisic acid inhibits type 2C protein phosphatases via the PYR/PYL family of START proteins. *Science* 2009; **324**:1068-1071.
4 Ma Y, Szostkiewicz I, Korte A, *et al.* Regulators of PP2C phosphatase activity function as abscisic acid sensors. *Science* 2009; **324**:1064-1068.
5 Fujii H, Zhu JK. *Arabidopsis* mutant deficient in 3 abscisic acid-activated protein kinases reveals critical roles in growth, reproduction, and stress. *Proc Natl Acad Sci USA* 2009; **106**:8380-8385.
6 Soon FF, Ng LM, Zhou XE, *et al.* Molecular mimicry regulates ABA signaling by SnRK2 kinases and PP2C phosphatases. *Science* 2012; **335**:85-88.
7 Melcher K, Ng LM, Zhou XE, *et al.* A gate-latch-lock mechanism for hormone signalling by abscisic acid receptors. *Nature* 2009; **462**:602-608.
8 Miyazono K, Miyakawa T, Sawano Y, *et al.* Structural basis of abscisic acid signalling. *Nature* 2009; **462**:609-614.
9 Nishimura N, Hitomi K, Arvai AS, *et al.* Structural mechanism of abscisic acid binding and signaling by dimeric PYR1. *Science* 2009; **326**:1373-1379.
10 Santiago J, Dupeux F, Round A, *et al.* The abscisic acid receptor PYR1 in complex with abscisic acid. *Nature* 2009; **462**:665-668.
11 Yin P, Fan H, Hao Q, *et al.* Structural insights into the mechanism of abscisic acid signaling by PYL proteins. *Nat Struct Mol Biol* 2009; **16**:1230-1236.
12 Melcher K, Zhou XE, Xu HE. Thirsty plants and beyond: structural mechanisms of abscisic acid perception and signaling. *Curr Opin Struct Biol* 2010; **20**:722-729.
13 Hauser F, Waadt R, Schroeder JI. Evolution of abscisic acid synthesis and signaling mechanisms. *Curr Biol* 2011; **21**:R346-R355.
14 Wilkinson S, Hartung W. Food production: reducing water consumption by manipulating long-distance chemical signalling in plants. *J Exp Bot* 2009; **60**:1885-1891.
15 Morison JIL, Baker NR, Mullineaux PM, *et al.* Improving water use in crop production. *Phil Trans R Soc B* 2008; **363**:639-658.
16 Melcher K, Xu Y, Ng LM, *et al.* Identification and mechanism of ABA receptor antagonism. *Nat Struct Mol Biol* 2010; **17**:1102-1108.
17 Qian W, Miki D, Zhang H, *et al.* A histone acetyltransferase regulates active DNA demethylation in *Arabidopsis*. *Science* 2012; **336**:1445-1448.
18 Gong Z, Morales-Ruiz T, Ariza RR, *et al.* ROS1, a repressor of transcriptional gene silencing in *Arabidopsis*, encodes a DNA glycosylase/lyase. *Cell* 2002; **111**:803-814.
19 Fujii H, Chinnusamy V, Rodrigues A, *et al. In vitro* reconstitution of an abscisic acid signalling pathway. *Nature* 2009; **462**:660-664.
20 Xu ZJ, Nakajima M, Suzuki Y, *et al.* Cloning and characterization of the abscisic acid-specific glucosyltransferase gene from adzuki bean seedlings. *Plant Physiol* 2002; **129**:1285-1295.
21 Saito S, Hirai N, Matsumoto C, *et al. Arabidopsis* CYP707As encode (+)-abscisic acid 8'-hydroxylase, a key enzyme in the oxidative catabolism of abscisic acid. *Plant Physiol* 2004; **134**:1439-1449.
22 Otwinowski Z, Borek D, Majewski W, *et al.* Multiparametric scaling of diffraction intensities. *Acta Crystallogr A* 2003; **59**:228-234.
23 McCoy AJ, Grosse-Kunstleve RW, Adams PD, *et al.* Phaser crystallographic software. *J Appl Crystallogr* 2007; **40**:658-674.
24 Kleywegt GJ, Jones TA. Efficient rebuilding of protein structures. *Acta Crystallogr D Biol Crystallogr* 1996; **52**:829-832.
25 Emsley P, Cowtan K. Coot: model-building tools for molecular graphics. *Acta Crystallogr D Biol Crystallogr* 2004; **60**:2126-2132.
26 Brunger AT, Adams PD, Clore GM, *et al.* Crystallography & NMR system: A new software suite for macromolecular structure determination. *Acta Crystallogr D Biol Crystallogr* 1998; **54**:905-921.
27 Murshudov GN, Vagin AA, Lebedev A, *et al.* Efficient anisotropic refinement of macromolecular structures using FFT. *Acta Crystallogr D Biol Crystallogr* 1999; **55**:247-255.

(**Supplementary information** is linked to the online version of the paper on the *Cell Research* website.)